ARCHIVES
of
FOUNDRY ENGINEERING

ISSN (1897-3310)
Volume 16
Issue 1/2016

89 – 94

16/1

Published quarterly as the organ of the Foundry Commission of the Polish Academy of Sciences

Examining the Possibilities of Analyzing the Solidification Process of Al-Si Alloy with the Infrared Camera

R. Władysiak *, A. Kozuń, T. Pacyniak
Department of Materials Engineering and Production Systems, Lodz University of Technology,
Stefanowskiego 1/15 Street, 90-924 Łódź, Poland
* Corresponding author. E-mail address: ryszard.wladysiak@p.lodz.pl

Received 06.07.2015; accepted in revised form 17.07.2015

Abstract

The paper presents the results of the crystallization process of silumin by the TDA thermographic method and the results of the cast microstructure obtained in the sampler ATD-10, that was cooling down in ambient air. The study was conducted for silumins AlSi8 and AlSi11 unmodified. The work demonstrated that the use of thermal imaging camera allows for the measurement and recording the solidification process of silumin. Thermal curve was registered with the infrared camera and derivative curve that was calculated on the base of thermal curve have both a very similar shape to adequate them TDA curves obtained from measurements using a thermocouple. Test results by TDA thermographic method enable quantitative analysis of the kinetics of the cooling and solidification process of hypo- and neareutectic silumins.

Keywords: Innovative foundry technologies and materials, Thermography, TDA, Al-Si alloy, Microstructure

1. Introduction

This work is a continuation of research into the improvement of thermal and derivative analysis (TDA) in research the solidification process of metals and alloys. The paper presents the possibility of implementing ATD with a thermal imaging camera.

At the turn of the last few years, this method is still developing. New types of probes have been developed, new basic software of the methods as well as new control algorithms. This expands its application to the study of new types of metal materials [1-6].

Thermal and derivative analysis is carried out by an apparatus Crystaldigraph and a ceramic probe (e.g. ATD-10) with the thermocouple type K or S placed in the heat center of sample area. In the TDA method are recorded two curves: cooling $t = f(\tau)$ and crystallization $t' = dt/d\tau = f'(\tau)$. Crystallization phases during cooling of the melt causes specific for sample alloy stops of temperature on thermal curve reflected clear thermal effects (peaks and humps) on the derivative curve. Interpretation of the shape and the characteristic point values of the TDA curves allow the analysis of the solidification process and evaluate the quality of the liquid alloy casting.

Temperature measurement in the TDA method uses a thermocouple that is the basis for the calculation and registration of the curves. Its operation is based on the phenomena of occurrence of the point of connection of two different metals of the electromotive force, the magnitude of which depends on the temperature of the connector. This phenomenon has been noted and explained in the nineteenth century by Seebeck, Peltier and Thomson [7].

Currently, thermography is a very fast growing method allowing to track various processes that cause fixed and variable temperature field. The essence of the method is the assumption

that all of the solids, liquids and gases whose temperature is higher than absolute zero (0 K) emit radiation with energy dependent on temperature and wavelength of radiation [8].
Infrared thermography is involved in detection, registration, processing and visualization of invisible infrared light (heat) emitted by the tested object. An essential element of modern infrared cameras is microbolometer infrared detector converting a photon energy of infrared radiation into an electrical signal. The value of the received signal depends directly on the temperature of the object, lens type, size and resolution matrix detector. These modern cameras work with a high resolution matrix of and an advanced methods of reading infrared amplification, the current-voltage conversion (IU) and a correction of heterogeneity signal. These features enable them recording the high-resolution temperature field at several tens mK and frequency measurement order of 10^2 Hz [9].

2. Experimental

The research was conducted on a station, which schematically was shown in Figure 1. The station is equipped with a resistive melting furnace, Crystaldigraph PC (U/f converter + software) manufactured by Z-TECH, infrared camera PI OPTRIS 160, the probe ATD-10 shown in Figure 2, optionally equipped with a quartz glass piece and a computer PC to control and record obtained results. Determination of emissivity measurement was made using the comparative method, using a standard thermocouple. Microstructure of the samples was performed using a Nikon microscope MA200.

The examination of the solidification process of the silumin was carried out simultaneously by Crystaldigraph in the sampler ATD-10 and the infrared camera. During the tests the temperature measurement and recording of solidifying the sample of silumin performed using thermocouple S and by observation of the free surface of the metal sample - in the first variant and with use of the quartz piece - in the second variant. The tests were performed for AlSi8 and AlSi11 alloys, which chemical composition is shown in Table 1.

Table 1.
Chemical composition of AlSi8 and AlSi11 alloys

Alloy	Chemical composition, weight %								
	Si	Mg	Cu	Mn	Fe	Ti	P	B	Sr
AlSi8	7.81	0.024	0.034	0.132	0.276	0.007	-	-	-
AlSi11	12.84	0.516	0.042	0.037	0.173	0.016	0.001	0.0062	0.0001

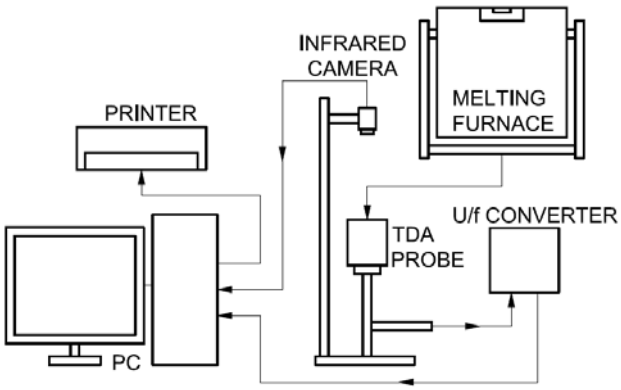

Fig. 1. Scheme of research station

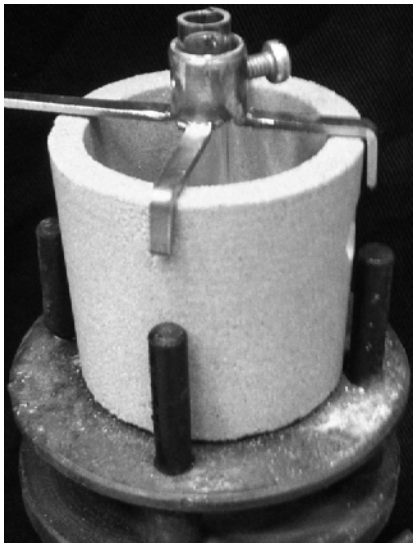
Fig. 2. View of ATD-10 probe with quartz glass piece

3. Results

The research was conducted with using hypo- and neareutectic silumins AlSi8 i AlSi11. Its composition is dominated by two elements, aluminum and silicon, wherein the silicon content may range from about 7÷13%. Basic reference of the subject demonstrates that the microstructure of the silumin group occurs only in a predominant amount, eutectic α + β (Al + Si). In the neareutectic silumin which has a much greater range of the solidification temperature, there is a additionally preeutectic crystallization of dendrites α (Al).

The amount of phases depends on the speed of growth, temperature gradient and chemical composition, which define the size and shape of the coupled growth zone.

In the Figure 3 TDA the observation of microstructure of tested samples shows that in both silumins there are grains of eutectic Al+Si (α+β) and dendritic of aluminum (α). AlSi11 alloy has also a single longwall (20÷50μm) separation of silicon (β) which crystallized preeutectically.

Figure 4 shows the results of the solidification process of AlSi8 silumin by TDA method.

The analysis of the chemical composition and microstructure observation of silumin shows that the solidification starts from the nucleation of aluminum. The maximum thermal effect is reflected in the form of a clear peak with a maximum cooling rate $dt/d\tau$ = 0.37 °C/s at A at the temperature tA = 609°C.

In the micro-regions remaining liquid around the dendrites of aluminum the silicon concentration increases. After supercooling of the liquid below the eutectic transition temperature tC = 581°C, silumin enters into a zone of coupled growth of eutectic. In the CDEF range the irregular lamellar eutectic crystallizes. This process is stabilized at tE = 582°C. Crystallization of the silumin ends at tF = 524°C.

In the case of silumin AlSi11 (Fig. 4 c), crystallization of eutectic α + β (Al + Si) is preceded by preeutectic separation of a small amounts of β-phase (Si) and α (Al) in the micro-regions of the sample. The research shows that the small rate of liquid silumin cooling about 3°C/s and average cooling rate of the alloy solidification temperature range is equal 0.14 °C/s may result in eutectic silumin the crystallization of primary Al and Si crystals. besides the eutectic grains.

Figure 5 shows the display screen with the selected thermographic test results using a thermal imaging camera, the surface area of the free silumin AlSi8 solidifying in the sampler ATD-10. Figure includes a plot of the maximum temperature at the time of the free surface area of the "Area 1", the thermogram of the sample surface, the strip temperature and the reference histogram temperature distribution with the mean value and standard deviation of this distribution.

The study also analyzed the value of the maximum temperature in the middle of the field "Area 1" with dimensions reduced to a few pixels. The results recorded in this way the temperature $t = f(\tau)$ and the calculated derivative $t' = dt / d\tau = f'(\tau)$ for silumin AlSi8 shown in Figure 6. The research shows that in the initial stage there is a rapid cooling of the temperature drop, which is caused by the reaction of the liquid metal with the air and changes: physical state, roughness and shape of the surface layer of the sample.

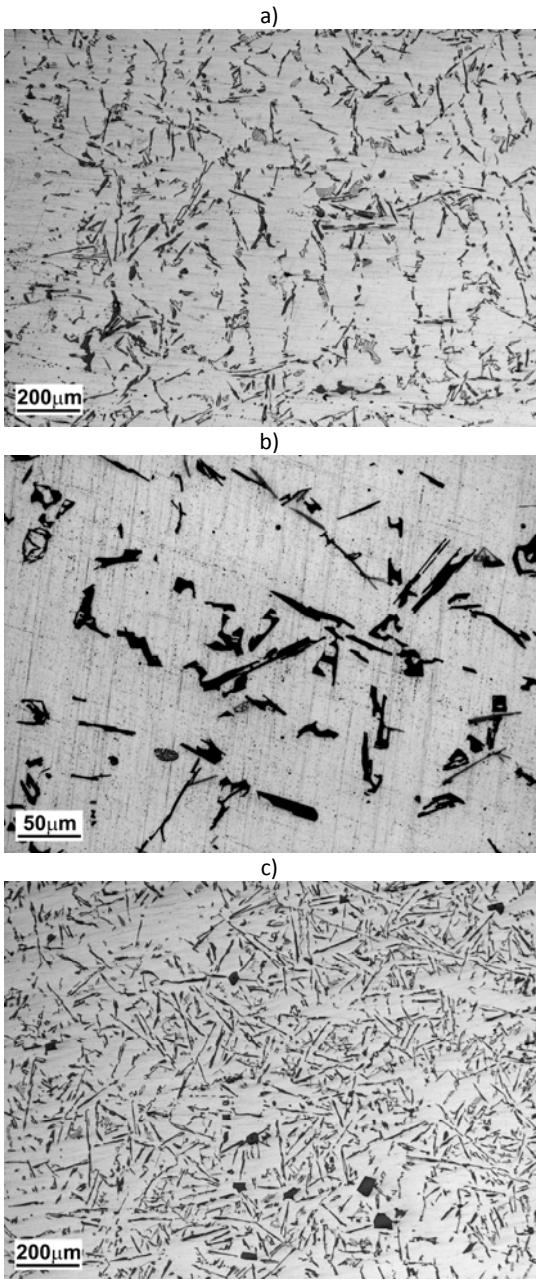

Fig. 3. Microstructure of probe casting made of AlSi8 (a, b) and AlSi11 (c) alloys. Structure: dendrites Al (a-c), lamellar eutectic grains Al+Si (a-c), walled crystals Si (c)

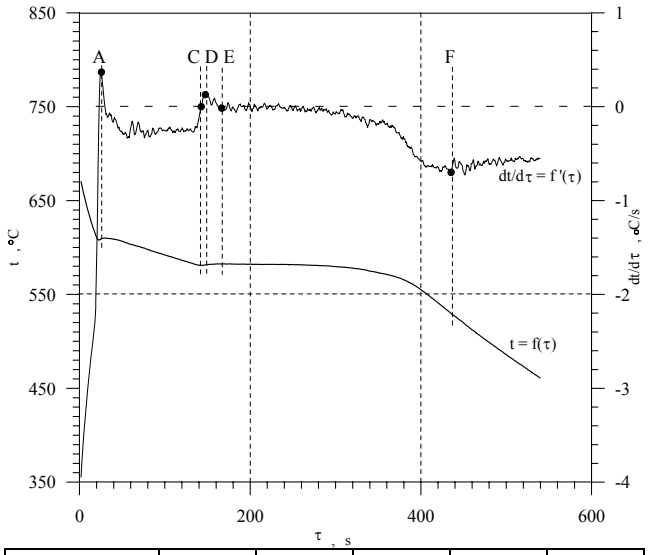

	A	C	D	E	F
t, °C	609	581	580	582	524
dt/dτ, °C/s	0.37	0	0.10	0	-0.69

Fig. 4. TDA curves and specific values of AlSi8 alloy solidification process

These changes cause a change in emissivity of the sample surface, the test surface by lowering the temperature to about 376°C.

In the next part of research the crystals of Al phase nucleate and grow preeutectically (Fig. 6: range AC) and after that the eutectic Al+Si crystallizes (Fig. 6, the range CF). As a result of emission of a latent heat from the crystallizing phases, the temperature of the entire metal sample, including the sample surface is increased to 571°C.

The analysis of the derivative curve (Fig. 6: $dt/d\tau=f'(\tau)$) shows that measure the surface temperature of the sample reflects the nature of the thermal processes taking place in the silumin, although the temperature and volume of the thermal effects do not correspond to the changes occurring within the sample solidifying metal.

In order to observe the thermal changes of silumin in the heat center of the probe were applied the probes with the quartz element (Fig. 2). Figure 7 shows the thermogram of the AlSi8 silumin test using a probe just like that.

The research shows that the temperature field defined by the quartz element is characterized by high homogeneity and stability of indications. Enhancing the quality of measurements of temperature values has a positive effect on the quality of the cooling curve and the results of the derivative curve calculation.

Figures 8 and 9 show TDA curves of AlSi8 and AlSi11 alloys obtained by using the probe of the quartz element and a thermal imaging camera.

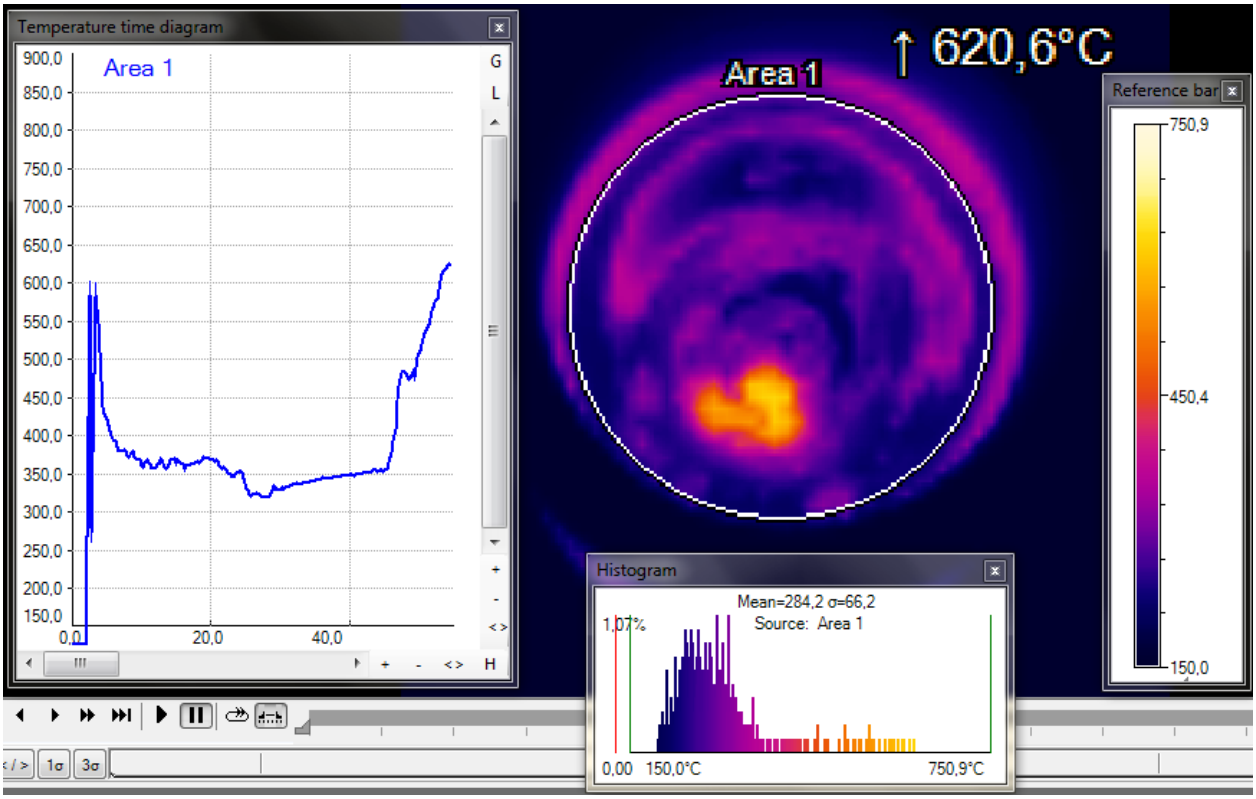

Fig. 5. Thermographic test results of the AlSi8 alloy in the ATD-10 probe

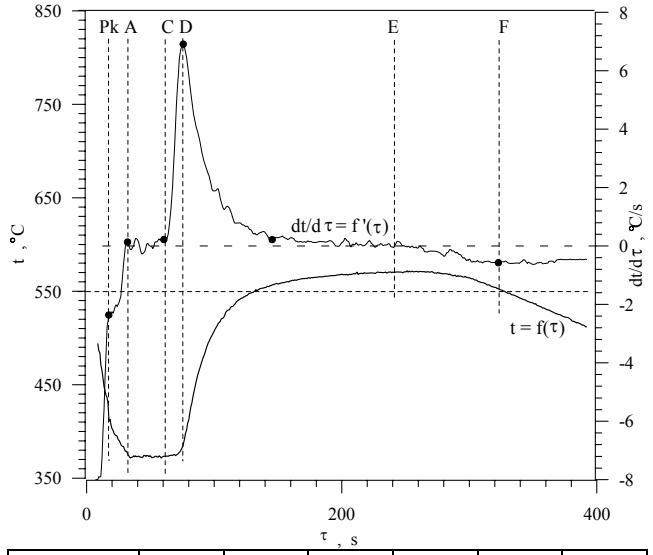

	Pk	A	D	E	F	G
t, °C	412	376	381	571	568	551
dt/dτ, °C/s	-2.31	0.11	0.69	0.24	-0.12	-0.59

Fig. 6. TDA curves and specific values of AlSi8 alloy solidification process using the thermographic method

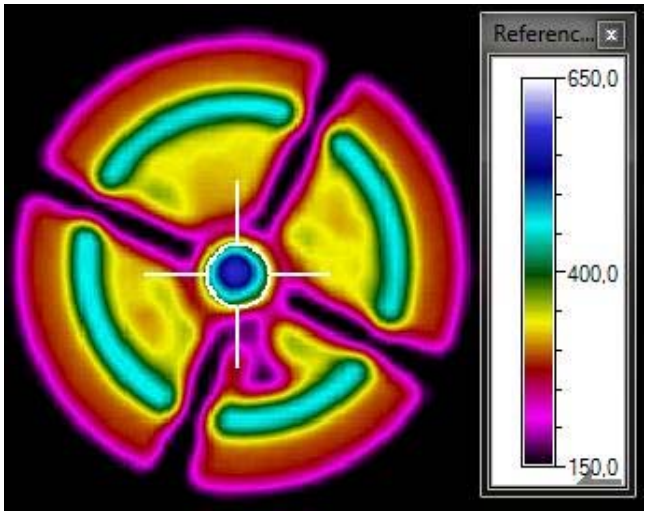

Fig. 7. Thermogram of AlSi8 alloy sample achieved in the probe with quartz element

The study shows that the cooling curves obtained of the silumins have a course similar to the curves obtained by the TDA classical method with use a thermocouple for the temperature measurement. In addition, they suggest that the definition of analyzed temperature fields using the quartz element placed in the heat center eliminates the problems caused by phenomena occurring on the free surface of the metal.

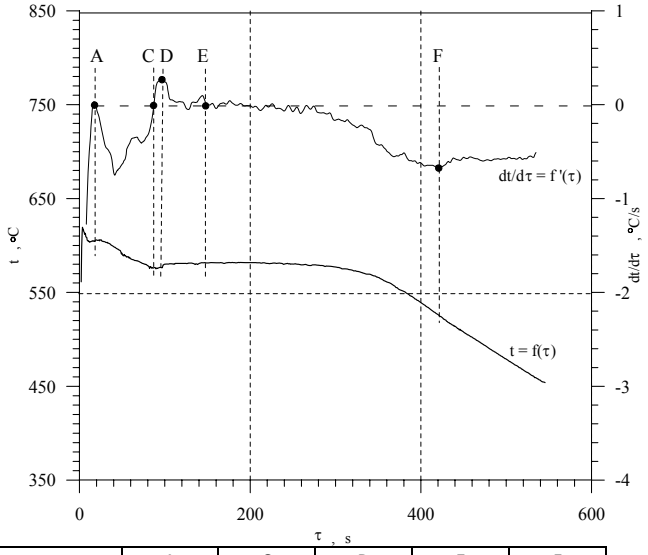

	A	C	D	E	F
t, °C	606	577	575	581	524
dt/dτ, °C/s	0.08	0	0.28	0	-0.78

Fig. 8. TDA curves and specific values of AlSi8 alloy solidification process using the thermographic method and the probe with quartz element

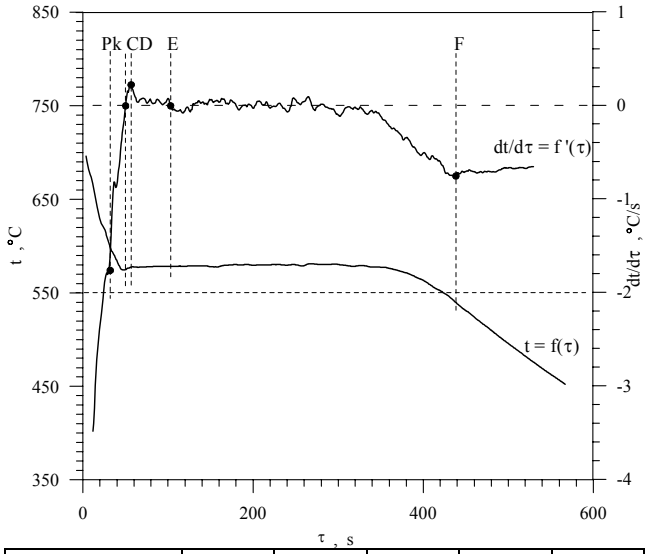

	Pk	C	D	E	F
t, °C	590	575	578	579	533
dt/dτ, °C/s	-1.84	0	0.24	0	-0.68

Fig. 9. TDA curves and specific values of AlSi11 alloy solidification process using the thermographic method and the probe with quartz element

A comparison of the temperature of characteristic points of the AlSi8 thermal curves shows that there are tiny differences in the range of 1÷3°C. On the derivative curves (dt / dτ = f '(τ)) test results using TDA (Fig. 4) and thermographic method (Fig. 8, 9)

there are analogous thermal effects of crystallizing phases of preeeutectic and eutectic stage (Al + Si) as well.

A thermal imaging method shows also the kinetics of the preeutectic and eutectic maximum thermal effect properly $(dt/d\tau)_A$=0.08°C/s, $(dt/d\tau)_D$=0.28°C/s. From comparing to the method of TDA (Fig. 4) follows that these specific values are less in the preeutectic range $(dt/d\tau)_A$=0.37°C/s and higher in the eutectic $(dt/d\tau)_D$ = 0.10°C/s. The end of silumin crystallization is identified in both methods like cooling rate value $(dt/d\tau)_F$=(-0.69÷-0.78)°C/s.

In summary, the studies demonstrate that the use of thermal imaging camera allows for the measurement and recording of cooling and solidification process of silumins. Thermal curves and calculated on the basis the derivative curve have a very similar shape to the curves of TDA obtained from the thermocouple measurements. Results of studies by TDA thermographic method allow quantitative analysis of the cooling process kinetics of hypoeutectic silumin and neareutectic as well.

4. Conclusions

The study shows that:

- TDA thermographic method provides a quantitative analysis of kinetics of cooling and solidification process of hypo- and neareutectic silumins,
- tested methods of analysis the solidification process have similar values of the temperature and cooling rate at characteristic points of the process,
- analysis of the temperature field of free surface sample reflects the stages of solidification process occurring in the silumin.

References

[1] Jura, S. (1992). Calorimetric Curve in Thermal and Derivative Analysis of the Crystallization Process. *Solidification of Metals and Alloys.* 17, 39. (in Polish).

[2] Jura, S. & Jura, Z. (1996). The theory of ATD method in the study of Al alloys. *Solidification of Metals and Alloys*. 28, 57. (in Polish).

[3] Pietrowski, S., Pisarek, B. & Władysiak, R. (1998). Alloy cast iron with vermicular graphite. *Solidification of Metals and Alloys*. 37, 105. (in Polish).

[4] Władysiak, R. (2001). Austenitic cast iron control by ATD method. *Archives of Foundry*. 1(2/2), 400-407 (in Polish).

[5] Pietrowski, S. (2001). *Silumins*, Lodz: LUT Publishing House. (in Polish).

[6] Pietrowski, S., Gumienny, G., Pisarek, B. & Władysiak, R. (2005). Monitoring of production and quality control of casting alloys with use of ATD methods. *Archives of Foundry*. 5(15), 310-328.

[7] Michalski, L., Eckersdorf, K. (1986). *The temperature measurements.* Warszawa WNT, (in Polish).

[8] Więcek, B., De Mey, G. (2011). *Infrared Thermovision. Fundamentals and applications,* Warsaw: PAK Publishing House. (in Polish).

[9] Orżanowski, T., Madura, H., Powiada, E. & Pasierbiński, J. (2006). Analysis of the reading to the microbolometer detector matrix. *Measurement Inspection Automation*, *9*. (in Polish).